PHOTOCHEMISTRY OF BREVETOXIN, PbTx-2, PRODUCED BY THE DINOFLAGELLATE, *KARENIA BREVIS*

Jaclyn Pitt

A Thesis Submitted to the University of North Carolina at
Wilmington in Partial Fulfillment
Of the Requirements for the Degree of
Master of Science

Department of Chemistry and Biochemistry

University of North Carolina, Wilmington

2007

Approved by

Advisory Committee

_____ _____

_____

Accepted by

_____
Dean, Graduate School

TABLE OF CONTENTS

ABSTRACT

The predominant brevetoxin produced by *Karenia Brevis,* PbTx-2 was added to 0.2 µm-filtered Wrightsville Beach, North Carolina seawater (WBSW) and irradiated under simulated sunlight for six hours to determine its photolability. The average first order rate constant of PbTx-2 degradation was 0.20 ± 0.05 h^{-1} at 25 ºC. When PbTx-2 was added to UV-irradiated WBSW, the average rate constant decreased significantly to 0.08 ± 0.03 h^{-1} at 25 ºC relative to that of untreated WBSW suggesting dissolved organics are involved in the photodegradation of PbTx-2 in seawater. UV-irradiated WBSW treated with Chelex-100 resin to remove trace metals caused no degradation of PbTx-2 upon exposure to sunlight suggesting that trace metals, in addition to organics, are involved in the photodegradation of PbTx-2. Irradiation of PbTx-2 in deoxygenated filtered WBSW caused the toxin to degrade almost immediately upon exposure to simulated sunlight. The effect of deoxygenation on the photodegradation of other brevetoxins including PbTx-1, 3, 6 agreed with the rate of PbTx-2. PbTx-9 and the naturally-produced compound, brevenal, degraded considerably in deoxygenated WBSW but not as rapidly. These results demonstrate that photosensitizers are involved in the degradation mechanism, suggesting that PbTx-2 degrades by secondary photochemical pathway. The mechanism suggested here is that PbTx-2 degrades in the presence of the excited chromophoric dissolved organic matter (CDOM)* and trace metal complex. Furthermore, the removal of oxygen from seawater causes the rate of degradation to increase rapidly because (CDOM)* no longer scavenges oxygen thereby scavenging solely PbTx-2. A model is also proposed which suggests that 75% of PbTx-2 in coastal seawater can be removed in 6 hours by exposure to sunlight. This represents a significant impact on the residence time of the toxin in bloom indicating photodegradation is an important and perhaps the dominant sink of the toxin in coastal seawater.

ACKNOWLEDGEMENTS

I would like to thank my advisors, Drs. Robert Kieber, Stephen Skrabal, and Jeffrey Wright for their relentless support and guidance on this research. I would like to thank Dr. Kieber for making this process less financially stressful. Also, to my mentor, Thomas Schuster, for teaching me the inner workings of mass spectrometry as well as laboratory practice, and for also being a great friend. Thanks especially to Carrie Miller, Andrea Bourdelais, and Ryan Van Wagoner for their patience and support with my random questions throughout the past year. Also, I'd like to thank the MACRL group for entertaining me and letting me entertain them during those long days at the laboratory. Without this group, this experience would not have been nearly as fulfilling and enjoyable. Finally, thanks to the Marine Science department for truly providing me with a well-rounded, challenging, and intriguing education.

LIST OF TABLES

LIST OF FIGURES

Page

INTRODUCTION

The marine dinoflagellate, *Karenia brevis*, can form harmful algal blooms known as red tides along the southern Atlantic coast and the Gulf of Mexico. These events occur almost annually in Florida's Gulf coastal waters, but have also been reported from Florida's eastern coast, North Carolina, northern Spain, Japan, and New Zealand (Baden et al. 1995; Baden et al. 2005; Cheng et al. 2005). *K. brevis* produces a series of potent neurotoxins known as brevetoxins. These toxins can accumulate in shellfish, and ingestion of contaminated shellfish results in a syndrome known as neurotoxic shellfish poisoning in humans which leads to gastrointestinal and neurological afflictions (Kirkpatrick et al. 2004). Symptoms induced by NSP may include nausea, cramps, parasthesis of the lips, face, and extremities, paralysis, seizures and coma (Baden et al. 1982). These toxins are also responsible for killing millions of fish (Forrester et al. 1977), birds, mammals, and other marine organisms that ingest or inhale the toxin (Bossart 1998). The Red Tide Research Program has conducted ongoing studies for the past decade on volunteers exposed to red tide events. Concentrations of brevetoxins determined by this program are 0.05-28 μg L^{-1} in water and 1.3-27 ng m^{-3} in air near bloom areas (Backer et al. 2005; Cheng et al. 2005). As cells of *K. brevis* lyse, brevetoxins can aerosolize by wind and wave action, resulting in respiratory and eye irritations in marine mammals and humans (Pierce et al. 1986; Pierce 2003). Air concentrations as low as 3-4 ng m^{-3} can cause irritation in the upper respiratory tract, itchy eyes, and coughing (Cheng et al. 2005). *K. brevis* occur naturally in the Gulf of Mexico at an abundance of < 1000 cells L^{-1} during non-bloom events, but can reach thousands to millions of cells L^{-1} during bloom events creating highly toxic conditions (Pierce et al. 2001).

Brevetoxins are a family of lipophilic trans-fused cyclic polyethers with *syn* relative stereochemistry, based on two structural backbones denoted A and B (Figure 1), with a molecular weight range of 800-1050 g mol^{-1} (Lin et al. 1981; Shimizu et al. 1990). Toxins are labeled PbTx-1 through PbTx-14 (Backer et al. 2003). PbTx-2 (type B) and PbTx-1 (type A) are the parent toxins

whereas the remaining identified toxins are considered to be derivatives (Baden et al. 2005). Using molecular modeling, Rein et al. (1994) and Gawley et al. (1995) established that both PbTx-1 and PbTx-2 are relatively linear molecules with a slight bend at approximately mid-molecule. Three regions of the structural backbone include the A-ring labeled the "head" which exhibits lactone functionality, the slightly flexible B-G rings known as the "spacer region," the terminal H-K ring in PbTx-2 and G-J ring in PbTx-1 labeled the "rigid region", and a highly reactive alpha beta unsaturated aldehyde side chain known as the "tail" region (Gawley et al. 1995) (Figure 1). These structural characteristics cause the large toxins to disrupt the normal function of voltage-sensitive sodium channels (VSSC) (Trainer et al. 1994). A normal VSSC opens due to cell membrane depolarization followed by inactivation in the late phase after initial activation (Baden et al. 2005). The channel then closes during membrane repolarization. The H-K region of all active brevetoxins binds to site 5 on the alpha subunit of a voltage-sensitive sodium channel (Poli et al. 1986). The toxins orient themselves "head" down into the sodium channel (Gawley et al. 1995) and sit between the alpha helices of domains III and IV of the VSSC (Trainer et al. 1994). The toxin causes the activation potential of the VSSC to shift to more negative values causing the channel to open at normal resting potentials. Also, the A-ring lactone extends the mean "open" time of the channel allowing for abnormal ion exchange through the cell membrane followed by inhibition of inactivation to return the channel from open to the inactive state, as well to induce subconductance states (Jeglitsch et al. 1998; Purkerson-Parker et al. 2000).

Each of the toxins exhibits varying binding affinities and toxicity. Binding affinities in synaptosome binding assays are PbTx-1>PbTx-3>PbTx-2>PbTx-6, therefore PbTx-1, PbTx-2, and PbTx-3 are considered the most potent toxins produced by *K. brevis* (Gawley et al. 1995). Hydrogen bonding of the A-ring carbonyl of the "head" region to site 5 of the VSSC is the mechanism by which these toxins bind. It has been found that modification of the A-ring or A-ring carbonyl considerably alters the binding affinity and toxicity of the molecule (Gawley et al. 1995).

Also, modifications to the K and J-ring tails, as well as the conformation of the H-ring from boat-chair to crown, has also shown a distinct change in binding affinity and toxicity of brevetoxin B (Gawley et al. 1995; Rein and Borrone 1999; Purkerson-Parker et al. 2000).

Despite this documented toxicity and threat to marine and human life, the fate of brevetoxins after they are released into the water column after cell lysis is poorly understood. Well studied sinks of brevetoxins include biological uptake and metabolism, aerosol formation, and sedimentation. An additional sink, which has been shown to be important for the blue-green algal toxins, microcystins and for the marine toxin domoic acid, is photodegradation (Welker and Steinberg 2000; Bouillon et al. 2006). Understanding the biogeochemical cycling of brevetoxin is particularly important because degradation products of brevetoxins may be even more toxic than the parent compounds. It is possible that the photochemical reactions involving brevetoxins may change the residence time or toxicity of natural bloom events.

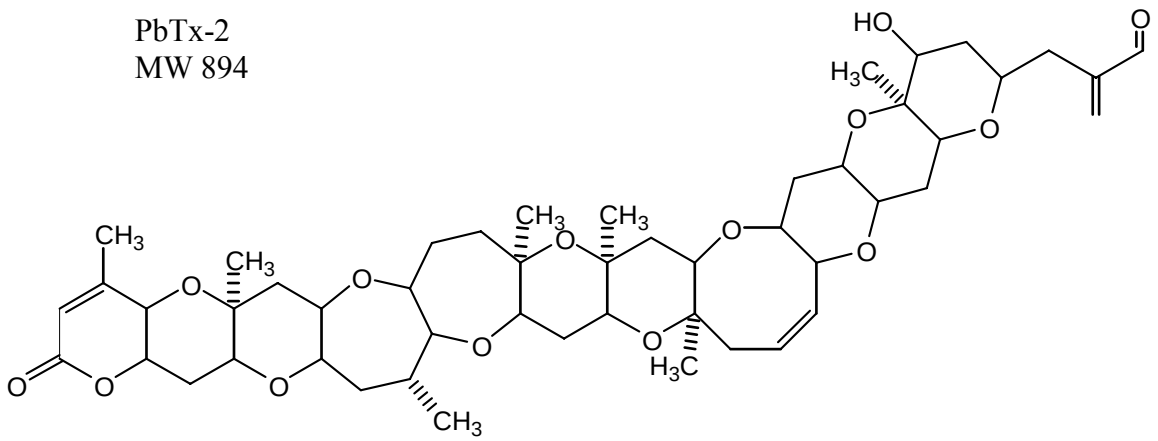

Figure 1. Type B (PbTx-2), one of the parent structural backbones of the family of brevetoxins.

Sunlight-mediated processes can initiate both direct and indirect photochemical transformations (Zafiriou et al. 1984). According to the first law of photochemistry, photons must be absorbed in order for a photochemical reaction to occur (de Mora et al. 2000). Direct photochemical reactions alter the substance which absorbs light. Indirect reactions transform naturally occurring sensitizers, such as chromophoric dissolved organic matter (CDOM), in the water column which can subsequently react with non-photosensitive substances in the environment (Mill 1999). For example, irradiation of CDOM produces hydroxyl radicals which may then interact with other compounds within the sample to cause photodegradation (de Mora et al. 2000). The rate of a photochemical reaction is the product of the rate of light absorption and quantum yield. Quantum yield of a photochemical reaction is defined as the ratio of the number of molecules formed or degraded per number of photons absorbed by the system (Mill 1999). Brevetoxins have several possible photoreactive sites based on comparison with other photosensitive molecules including double bonds, a conjugated vinylic methylene group and two carbonyl groups (Baden and Tomas 1989). Brevetoxins are produced in the photic zone, and consequently are exposed to sunlight that may result in their photodegradation. For example, irradiation of domoic acid, a toxin produced by the diatom *Pseudo-nitzschia* species, generates three geometrical isomers (Bouillon et al. 2006). In the case of brevetoxins, Hardman (2003) found that PbTx-2, one of the most abundant and toxic brevetoxins in naturally-occurring blooms, is indeed photolabile (Rein and Borrone 1999; Pierce et al. 2007). Hardman's research involved qualitatively observed photodegradation of high concentrations of brevetoxin in seawater and did not establish a rate constant for the degradation of PbTx-2. The objective of Hardman's work was to determine the nature of the photodegradation products whereas the research here focused on quantifying the rate of photochemical degradation of natural concentrations of PbTx-2 similar to those in typical bloom events. This work also assessed whether photodegradation is a direct or indirect process and the extent to which environmental

parameters (CDOM, metals, particles, dissolved oxygen) are important in controlling that degradation. Results obtained in this research project provide a better knowledge of the photochemistry of brevetoxins that will greatly improve our ability to assess their fate in the surface waters of the ocean.

METHODS

Reagents and Standards

All solvents were obtained from Fisher Scientific or VWR International and were HPLC grade unless otherwise stated. A Milli-Q Plus water system (Millipore, Bedford, MA) provided deionized water (>18.2 MΩ cm^{-1}) used for sample extraction and mobile phases. PbTx-2 (packaged under inert gas -20ºC; >95% purity; 100 µg) was obtained from World Oceans Solutions (Wilmington, NC). Each vial was rinsed with 1 mL acetone, transferred to an HPLC screw cap vial and stored at 4 ºC as a stock solution at a final concentration of 100 µg mL^{-1}. For each experiment, 1 mL of solution was evaporated to dryness with nitrogen gas and taken up to 1 mL volume with acetonitrile in preparation for analysis. Serial dilutions for standard curves were made from the stock solution in acetonitrile at concentrations of 1.1, 5.6, and 11.1 mM.

Photolysis Experiments

Seawater (salinity 32-34) was collected from Wrightsville Beach, NC (34.208º N, 77.796º W) in an acid cleaned 1 L glass container and filtered (0.2 µm acid cleaned filter) immediately to prevent bacterial growth. Filtered seawater (WBSW) was stored in the dark at 5 ºC until use. The pH of filtered seawater was measured with an Orion 8102 Ross combination electrode calibrated with NIST buffers. Irradiation solutions were spiked with an environmentally realistic concentration of PbTx-2 (Pierce et al. 2003). Filtered WBSW (450 mL) was spiked with PbTx-2 (0.11 µmol) and apportioned (25 mL) into each of 17 screw-cap quartz cells (30-cm long, 30 mL volume; Spectrocell, Inc.) to a final concentration of 240 nM in each cell. Twelve cells were placed vertically in a circular carrier and submerged in a

temperature controlled water bath (25 ºC) under a solar simulator (Spectral Energy Corp., LH 153 lamp housing, 1-kW Xe arc lamp, LPS 256 SM power supply, AM1 filter to remove wavelengths < 290 nm). Light measurements at individual cell locations were measured before and after photolysis (Ocean Optics SD2000 spectrophotometer, connected to fiber optic cable terminated with CC-UV cosine collector, calibrated with a NIST traceable tungsten lamp, data collected with OOIrad software). Three cells were placed in a dark cabinet at room temperature as controls. The solar simulator produced light similar to high noon, mid-summer solar irradiance at 34º N latitude (Figure 2). Duplicate irradiated samples were removed from the solar simulator and extracted for brevetoxin every hour for 6 h, whereas dark controls were extracted at 0, 3, and 6 h.

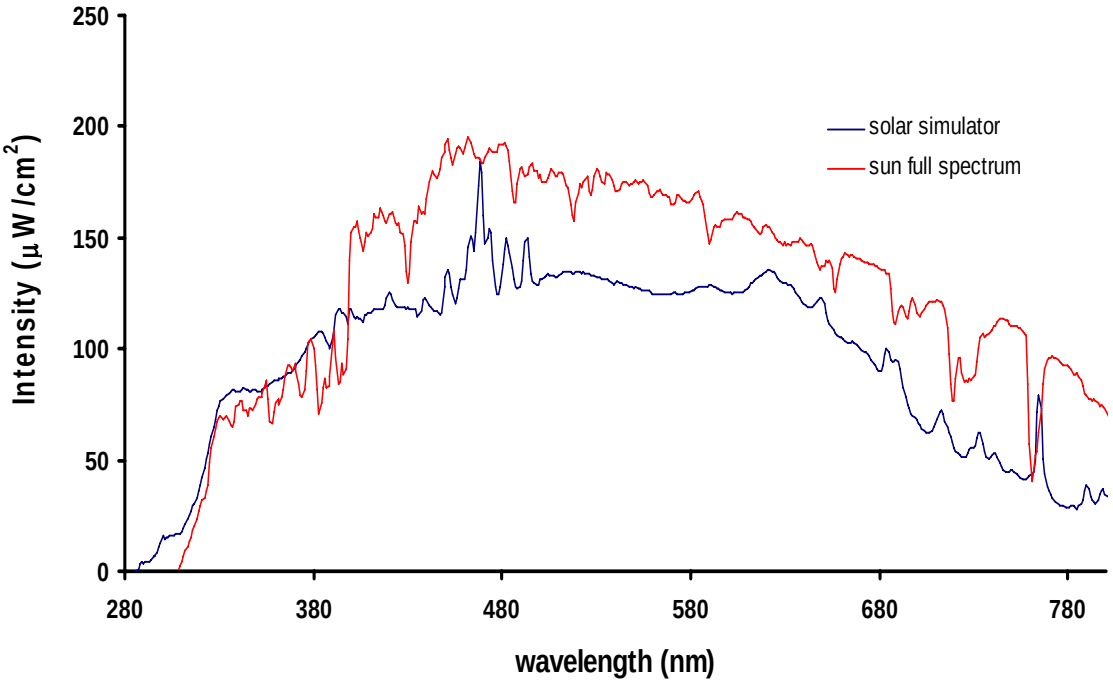

Figure 2. Intensity of light vs. wavelength of solar simulator vs. natural sunlight at high noon 35º N.

Sample Extraction

The highly hydrophobic nature of these toxins creates a very difficult substrate to manipulate in the laboratory setting. Therefore, all methods focused on minimizing contact of the toxin with glass and thorough elution was employed to remove all adhered toxin to materials such as pipettes, syringes, columns, and vessels. Several eluents and solid phase extraction cartridges were tested and analyzed by LCMS for optimal sample recovery (Table 1). Samples extracted with C_{18} reverse-phased cartridges and eluted with acetone yielded the highest percent recovery (92 ± 2 %, Table 1). Each C_{18} cartridge was washed with 6 mL acetone and 10 mL Milli-Q water prior to use. Samples were poured directly from the irradiation cell to the extraction device to mitigate loss of toxin. Samples were drawn drop-wise through the cartridge by vacuum (flow rate 1 mL min^{-1}). Each cartridge was washed with 10 mL Milli-Q water to remove salts and finally eluted with 6 mL acetone. Each sample was wrapped in foil and stored at 4 ºC until further analysis. Samples were vacuum-dried for 6 h, reconstituted with 1.5 mL of acetone and transferred to screw-capped HPLC vials. After drying with nitrogen gas, samples were reconstituted with acetonitrile to a final volume of 250 µL in preparation for analysis.

Liquid Chromatography Mass Spectrometry

PbTx-2 samples were analyzed by positive ion electrospray liquid chromatography mass spectrometry (QSTAR-XL, Applied Biosystems, Inc.). An optimized gradient elution (Table 2) was used (mobile phase A: 98% Milli-Q water, 2% acetonitrile; mobile phase B: 98% filtered ACN, 2% Milli-Q water, both with 0.1% formic acid, 0.01% trifluoracetic acid; Thomas Schuster, personal communication) through a reverse-phased C_{18} column (2.0 x 150 mm; 5 µm; Phenomenex, Torrance, CA), with an injection volume of 4.0 µL. Triplicate injections of each sample were alternated with a blank injection. A typical standard curve for 1.1 µM to 11.4 µM of PbTx-2 is shown in Figure 3. Response factors of each sample were compared to a standard curve generated from standard dilution series injected after each sequence. The counts per

second (CPS) at *m/z* 895.6 were converted to concentration based on the standard curve of its respective run.

Table 1. Percent sample recoveries of various tested cartridges and eluents. A sample of PbTx-2 spiked filtered WBSW (0.2 μm; 180 nM) was drawn through each cartridge. The percent recovery is an average (± 1 standard deviation) of 3 trials of each cartridge and eluent combination.

Cartridge	Eluent	% Recovery
C8	Acetone	80 ± 3
C8	Acetonitrile	72 ± 2
C8	Methanol	74 ± 4
C18	Acetone	92 ± 2
C18	Acetonitrile	81 ± 0.05
C18	Methanol	85 ± 3
C4	Acetone	76 ± 2
C4	Acetonitrile	73 ± 3
C4	Methanol	69 ± 1

Table 2. Parameters used for analysis of PbTx-2 by liquid chromatography mass spectrometry. a) Gradient used for liquid chromatography analysis. b) Source parameters used for mass spectrometry analysis. (Thomas Schuster, personal communication)

a)

Time (minutes)	% Mobile Phase A	% Mobile Phase B
0	40	60
10	10	90
13	40	60
30	40	60

b)

Source/Gas		Compound	
Ion source gas 1	30	Declustering Potential	65
Ion source gas 2	0	Focusing Potential	180
Curtain gas	25	Declustering Potential 2	15
Ionspray Voltage	5500		

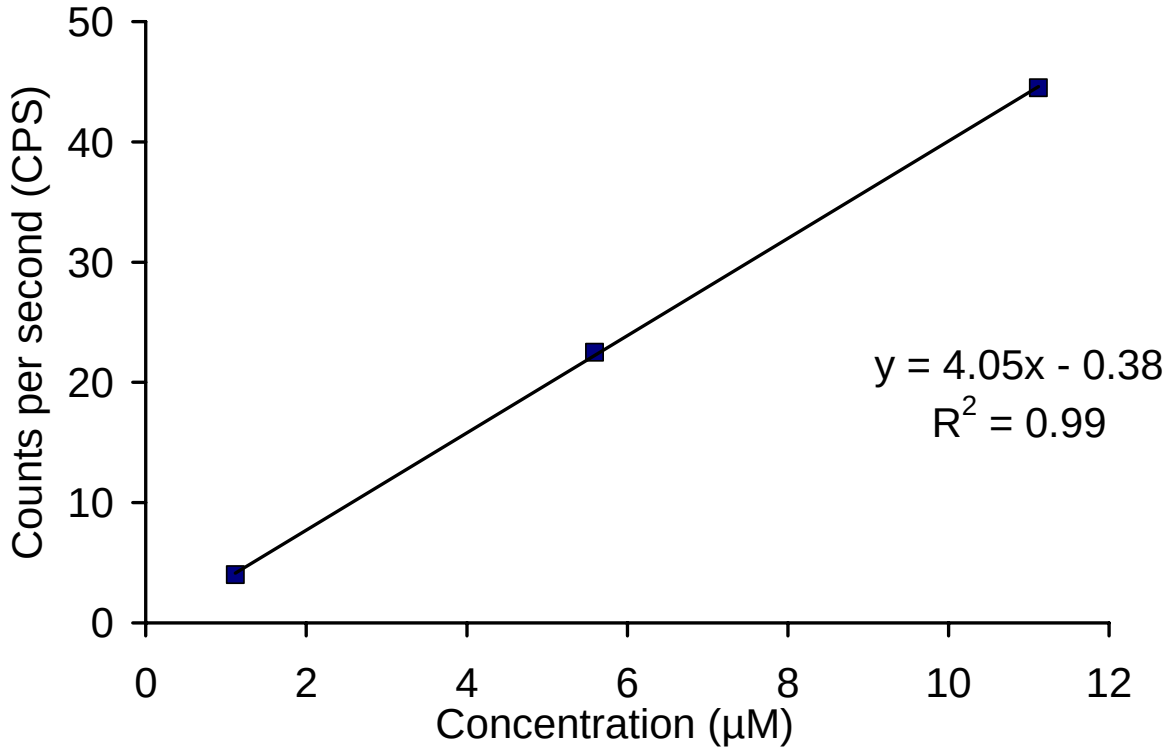

Figure 3. Counts per second as a function of concentration of PbTx-2 (µM) in a typical LCMS calibration curve.

Experimental Conditions

The first experimental manipulation was the removal of chromophoric dissolved organic matter (CDOM) from filtered WBSW by UV-oxidation (1200 W mercury vapor lamp, Ace Glass) of WBSW (0.2-μM). A portion of filtered WBSW (0.2 μm-filter; approx. 450 mL) was oxidized under UV light (5 h) and refrigerated (24 h) before photolysis. To begin the experiment, PbTx-2 (0.11 μmol) was spiked into a sample of UV-oxidized seawater (450 mL) to a final concentration of 240 nM in each cell. Aliquots of 25 mL were pipetted into each of 17 quartz spectrophotometric cells (10-cm long, 30 mL volume) and irradiated as described previously. Samples were then extracted and analyzed by LCMS. This experiment was repeated three times to determine an average rate constant for PbTx-2 photodegradation in UV-oxidized WBSW.

In order to investigate the role of trace metals and CDOM in PbTx-2 photodegradation, UV-oxidized WBSW was treated with Chelex-100 to remove trace metals. Filtered WBSW was UV-oxidized (3 h) then treated with Chelex-100 resin (20 g L^{-1}) and gently agitated overnight. The resin was allowed to settle (2 h), then the solution was filtered through an acid-washed polycarbonate filter (0.05 μm) using a trace metal clean filtering apparatus. The treated seawater was UV-oxidized again (3 h) to remove any organics leached from the resin and refrigerated (24 h) before photolysis. In preparation for these experiments, all glassware including quartz cells and pipette tips were soaked in 10% HCl for at least 24 hours and subsequently rinsed with Milli-Q water before use. Chelex-100 resin was cleaned before use by successive soakings in 6 M HCl and 2 M HCl (Trace Metal grade) and 1 M NH_4OH (Fisher Optima) with repeated rinsings of the resin with Milli-Q water between steps. Preparation of samples was carried out in a class 100 clean room with positive pressure to mitigate trace metal contamination. This experiment was carried out three times analogous to previous experiments and analyzed by LCMS.

Filtered WBSW was deoxygenated with nitrogen gas to determine the effect of oxygen and reactive oxygen species on the photodegradation of brevetoxin. Filtered WBSW (0.2-µm, 450 mL) was placed in a nitrogen-filled glove bag and bubbled with nitrogen gas (filtered, high purity) overnight. The pH of the seawater increased from 7.95 to 8.45 after bubbling, therefore diluted HCl was added to the seawater to return it to its original pH. PbTx-2 (0.11 µmol) was spiked into a deoxygenated sample (450 mL; adjusted to pH 7.95) of WBSW. Inside the glove bag, aliquots of the solutions were poured into quartz cells (30-cm long, 30 mL volume) to minimize headspace and capped. Samples were irradiated analogously to previous WBSW experiments, extracted, and analyzed by LCMS. An additional experiment was performed with PbTx-1, 2, 3, 6, and 9 (provided courtesy of Dr. Andrea Bourdelais, Center for Marine Science) to determine the effect of deoxygenation on the most common toxins found during bloom events (Bourdelais et al. 2005) (Figure 4). A sample of untreated filtered WBSW (0.2 µm, 125 mL) and deoxygenated filtered WBSW (0.2 µm, 125 mL) were simultaneously spiked with 35 µmol of each toxin. Each mixture, deoxygenated and oxygenated, was apportioned to 5 irradiation cells (30 cm-long, 30 mL volume). Due to availability of sample, time points were removed from simulated sunlight and extracted at 0, 3, and 6 h. Dark controls were extracted at 0 and 6 h to account for any non-photochemical degradation.

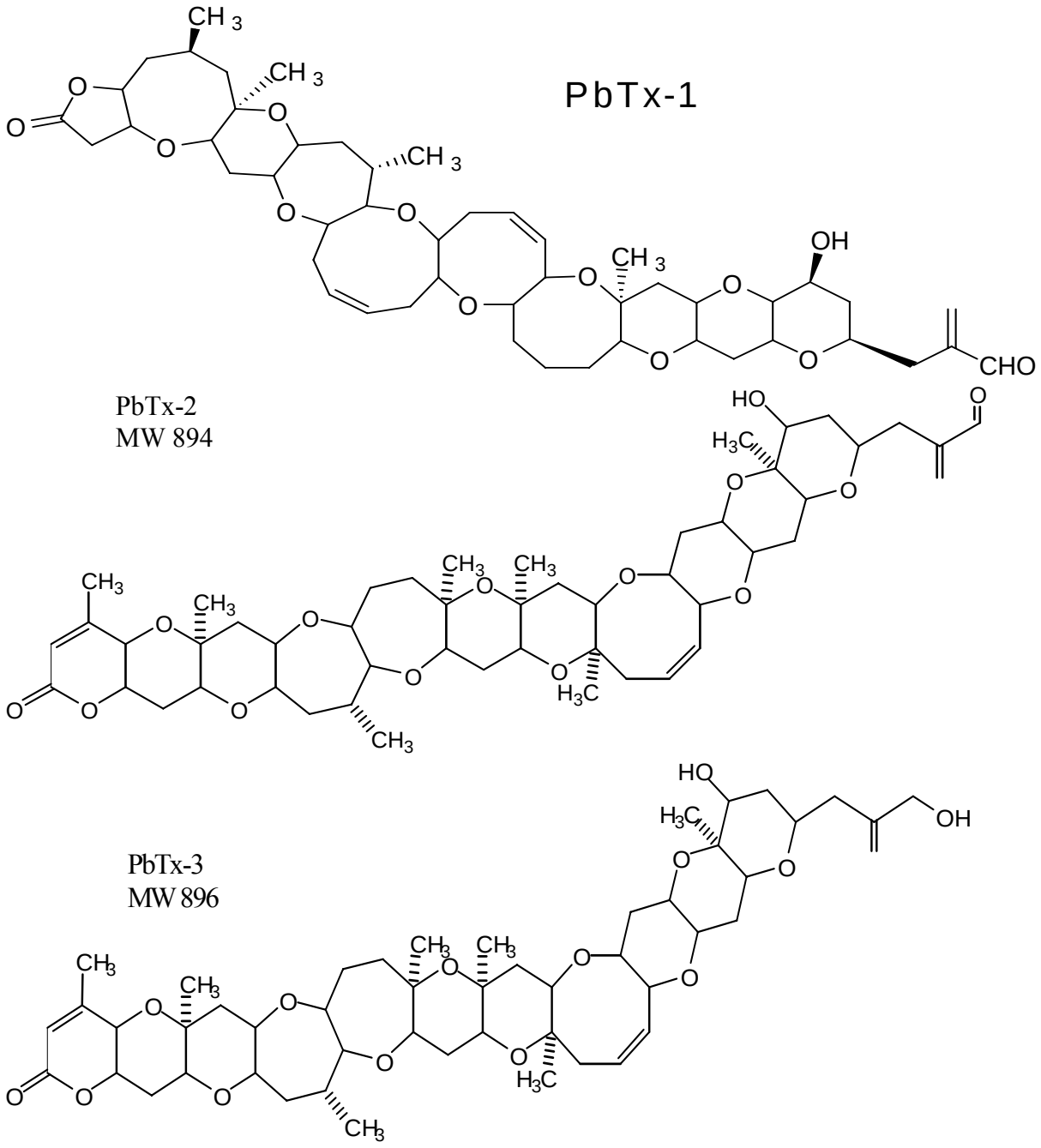

Figure 4. Structures of three common brevetoxins used in this study.

PbTx-6
MW 910

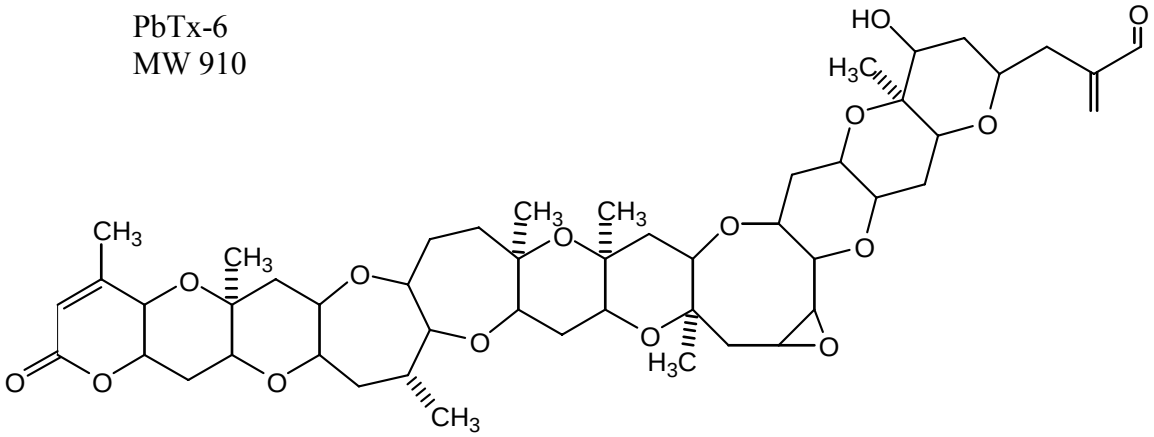

PbTx-3 42-carboxylic acid

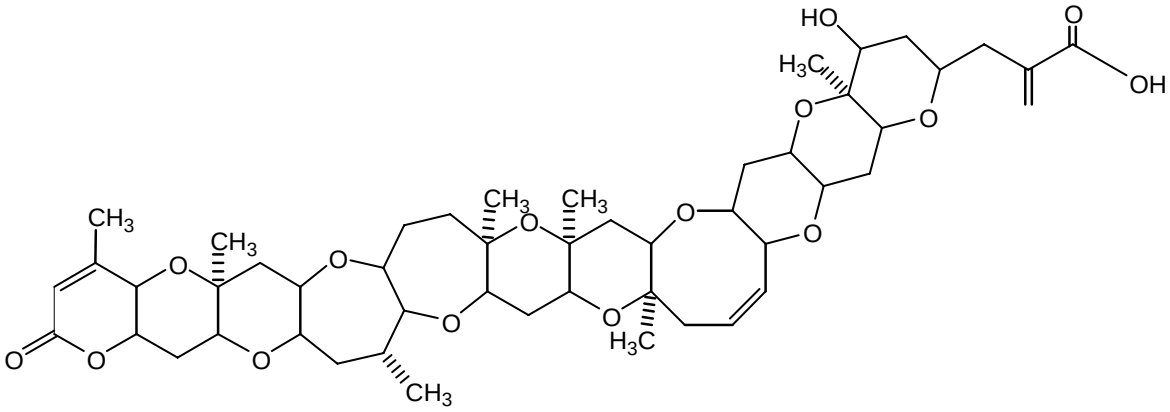

PbTx-9
MW 898

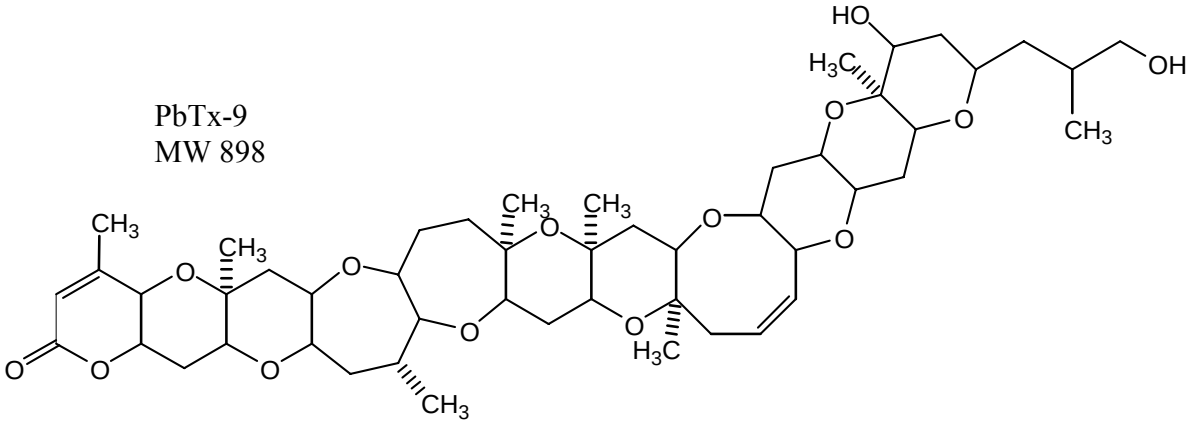

Figure 4 (continued): Structures of common brevetoxins used in this study.

To determine the rate of adsorption of PbTx-2 onto particles, two solutions, unfiltered and filtered WBSW, were spiked with a known concentration of PbTx-2. A volume of unfiltered seawater (250 mL) was spiked with PbTx-2 (0.05 µmol) and placed in a dark cabinet for 6 h. Filtered seawater (0.2-µm; 250 mL) was spiked with PbTx-2 (0.05 µmol) and also placed in a dark cabinet. Two aliquots (25 mL) of each solution were withdrawn at T=1 min., 6 h, and 24 h. Each sample was filtered (0.2 µm) and extracted with a C_{18} reverse phased cartridge. After 24 h, two 25 mL aliquots of each remaining solution were pipetted into quartz cells and irradiated for 6 h. Two aliquots (25 mL) of each sample were place in the dark for 6 h. After exposure, all samples were passed through a filter (0.2-µm) and extracted with a C_{18} cartridge. Extracted samples were prepared for analysis analogously to prior experiments and analyzed by LCMS.

RESULTS

Photodegradation of PbTx-2 in Filtered Coastal Seawater

The first objective was to establish a rate constant for the degradation of PbTx-2 in filtered WBSW (0.2-µm). A series of five photolysis experiments was carried out in WBSW at environmentally realistic concentrations. Initial experiments were conducted identically by spiking PbTx-2 (0.11 µmol) into a starting solution of filtered WBSW (0.2-µm; 450 mL) to a final concentration of 240 nM. Exposure of PbTx-2 to simulated sunlight for 6 h caused a loss in toxin whereas no loss of PbTx-2 was observed in the dark controls (Figure 5a). LCMS analyses for PbTx-2 yielded a peak (RT = 5.3 min) with a molecular ion at *m/z* 895.6. Loss of PbTx-2 was plotted as a pseudo-first order reaction in order to determine the rate constant of photodegradation (Figure 5b). Ten photolysis experiments at 25 ºC yielded an average rate constant of 0.20 ± 0.04 hr^{-1} (Table 3). As PbTx-2 decreased in concentration over a 6 h exposure, a suspected photodegradation product (*m/z* 911) increased in concentration as irradiation time progressed. This molecular ion is postulated to be the oxidized form of PbTx-2 in which the terminal aldehyde group is converted to a carboxyl group (Plakas et al. 2004),

although further characterization of this peak by NMR is necessary to confirm this assumption. Molecular ion (*m/z* 911) could also represent PbTx-6, the H-ring epoxide form of PbTx-2, which NMR would clarify as well (Hua and Cole 2000). Due to the lack of *m/z* 911 standard, the concentration of this molecular ion is expressed in PbTx-2 equivalents assuming the response of the two species is similar. Concentrations of PbTx-2 and molecular ion *m/z* 911 as a function of irradiation time are shown in Figure 6a. The plot of the natural logarithm versus time is shown in Figure 5b.

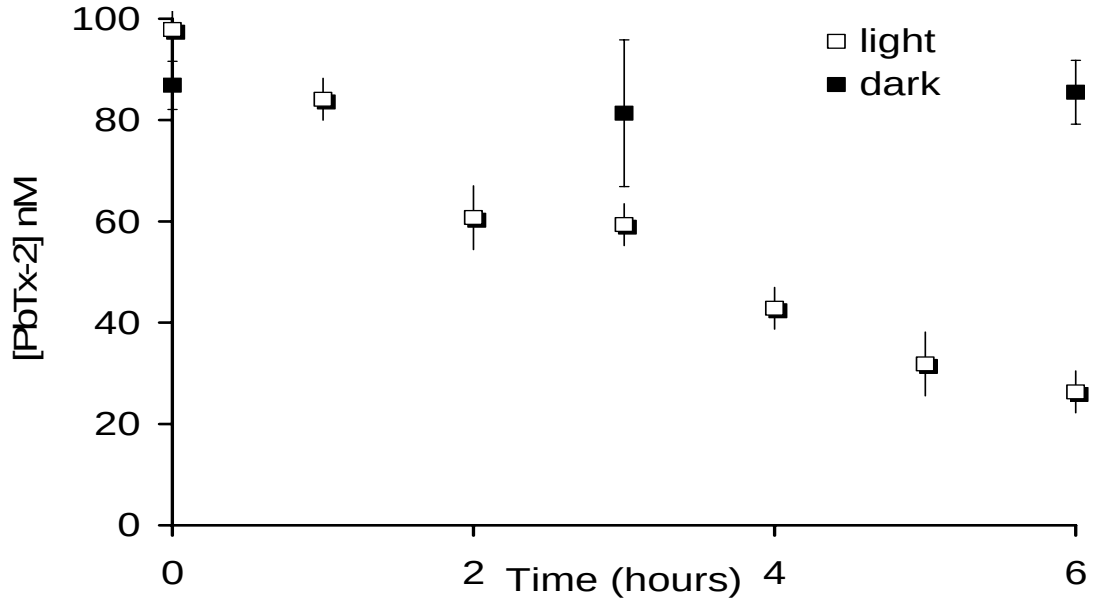

a.)

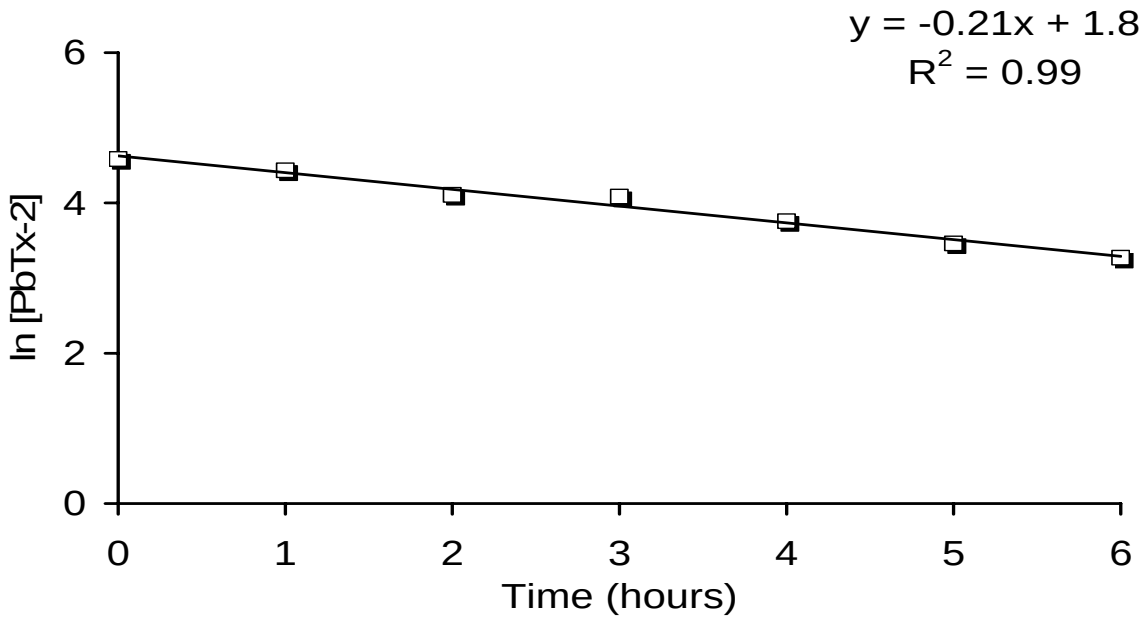

b.)

Figure 5: a) Loss of PbTx-2 concentration of light exposed and dark control samples as a function of irradiation time (hours) for one representative experiment. Error bars represent the standard deviation of triplicate LCMS injections per sample. B) Natural logarithm of the PbTx-2 concentration as a function of PbTx-2 as a function of irradiation time (hours). The line represents a best fit linear regression to the light exposed samples. Salinity 34, pH 7.95, temperature 25 ºC.

Table 3: Pseudo-first order rate constants of PbTx-2 in 0.2 μm filtered Wrightsville Beach seawater. A goodness of fit (R^2) is also shown for each plot of natural logarithm as a function of irradiation time. All samples were irradiated for 6 hours under simulated sunlight at 25 ºC.

Trial	**First Order Rate Constant (h^{-1})**	**R^2**
1	0.14	0.95
2	0.13	0.93
3	0.24	0.97
4	0.22	0.99
5	0.22	0.87
6	0.26	0.97
7	0.18	0.96
8	0.23	0.98
9	0.20	0.99
10	0.19	0.97
Mean ± std dev.	**0.20 ± 0.04**	

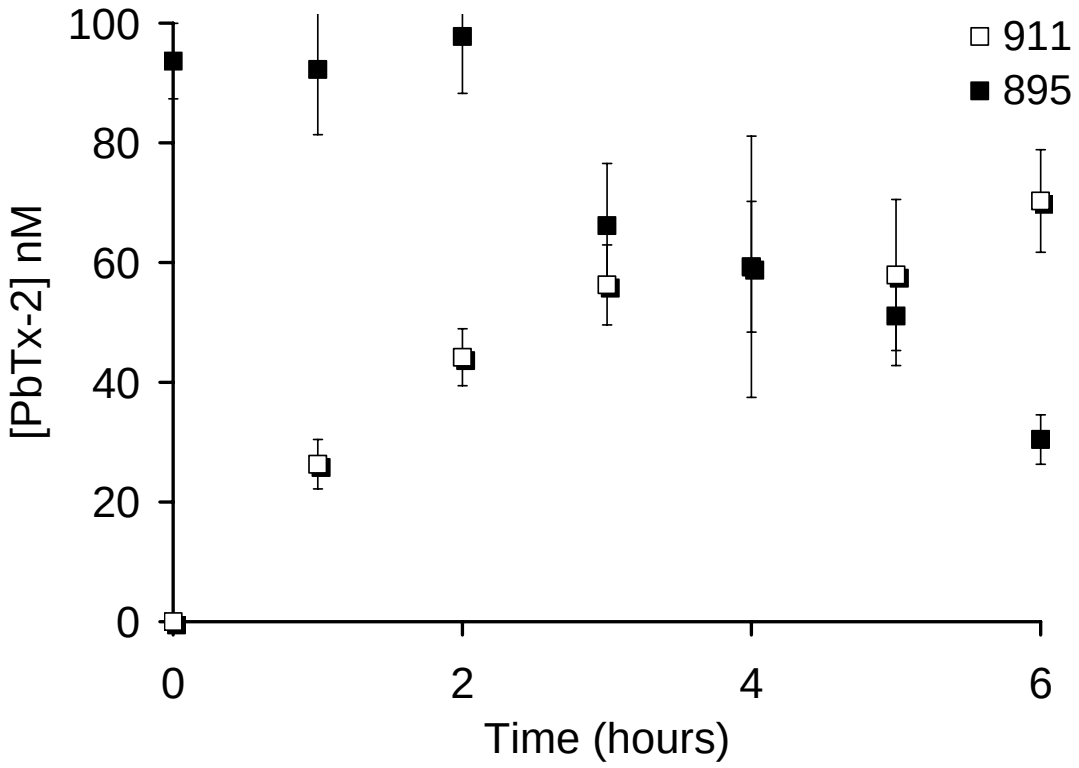

Figure 6: Loss of PbTx-2 (*m/z* 895) and gain of suspected photoproduct (*m/z* 911, expressed in PbTx-2 equivalents) as a function of irradiation time. The error bars represent standard deviations of triplicate LCMS injections of each sample.

Effect of Chromophoric Dissolved Organic Matter on PbTx-2 Photodegradation

A second series of experiments was conducted to determine how the presence of chromophoric dissolved organic matter (CDOM) affects the photodegradation of PbTx-2. Concentrations of PbTx-2 in filtered, UV-oxidized WBSW showed a loss of PbTx-2 whereas dark controls showed no loss (Figure 7a). Loss of PbTx-2 was plotted as a pseudo-first order reaction in order to determine the rate constant of photodegradation (Figure 7b). Five duplicate photolysis experiments established that PbTx-2 degraded about twice as slowly relative to non-irradiated seawater. These five photolysis experiments at 25 ºC had an average rate constant of $0.08 \pm 0.03\ h^{-1}$ (Table 4). The first order rate constant for the degradation of PbTx-2 was significantly different ($p = 0.0001$) than that of untreated WBSW (Mann-Whitney test; Systat 10.2). This suggests that CDOM significantly affects the rate at which PbTx-2 degrades in seawater.

a.)

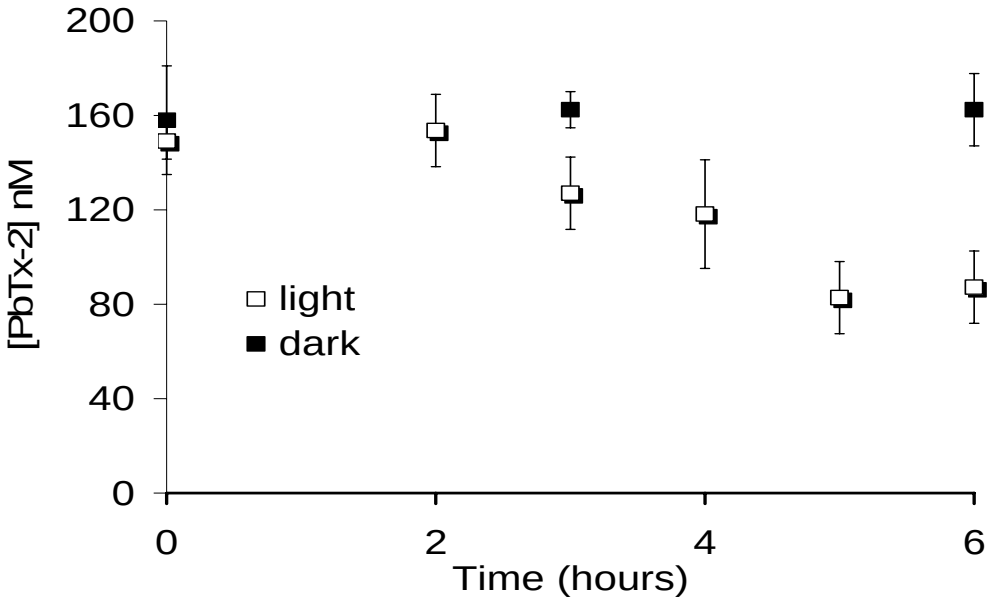

b.)

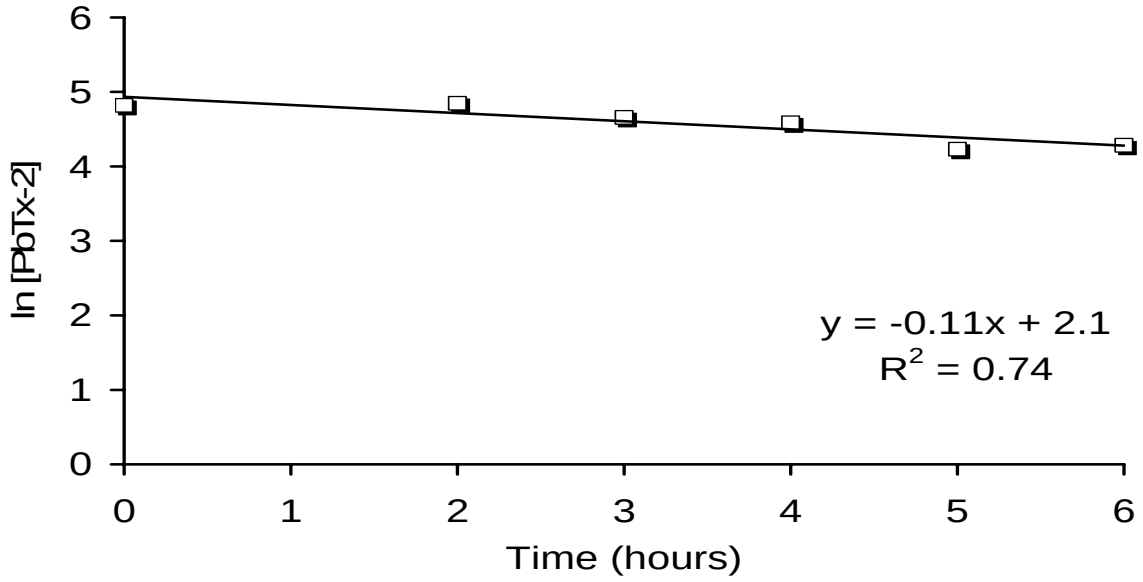

Figure 7: a) Loss of PbTx-2 concentration of light exposed and dark control samples as a function of irradiation time of one representative experiment in UV-irradiated 0.2 µm-filtered WBSW. Error bars represent one standard deviation of triplicate LCMS injections of each sample. b) Plot of natural logarithm of the PbTx-2 concentration as a function of irradiation time in hours in UV-irradiated 0.2-µm filtered WBSW. The line represents a best fit linear regression to the data. Salinity 34, pH 8.1, temperature 25 ºC.

Table 4: Pseudo-first order rate constants of PbTx-2 in UV-oxidized 0.2 µm filtered Wrightsville Beach seawater. The goodness of fit (R^2) is also shown for each plot of natural logarithm as a function of irradiation time. All samples were irradiated for 6 hours under simulated sunlight at 25 ºC.

Trial	**Pseudo-First Order Rate Constant (h^{-1})**	**R^2**
1	0.10	0.74
2	0.07	0.79
3	0.05	0.95
4	0.07	0.59
5	0.05	0.57
6	0.10	0.46
7	0.05	0.75
8	0.07	0.83
9	0.09	0.77
10	0.12	0.65
Mean ± st dev.	**0.08 ± 0.03**	

Effect of Trace Metals on PbTx-2 Photodegradation

A series of photochemical experiment was performed to determine the effects of trace metals naturally found in WBSW on the photodegradation of PbTx-2. Concentrations of PbTx-2 in UV-oxidized, trace metal clean, filtered WBSW showed no loss of PbTx-2 in both irradiated and dark samples (Figure 8). Degradation of PbTx-2 slowed significantly as compared to the first two experiments.

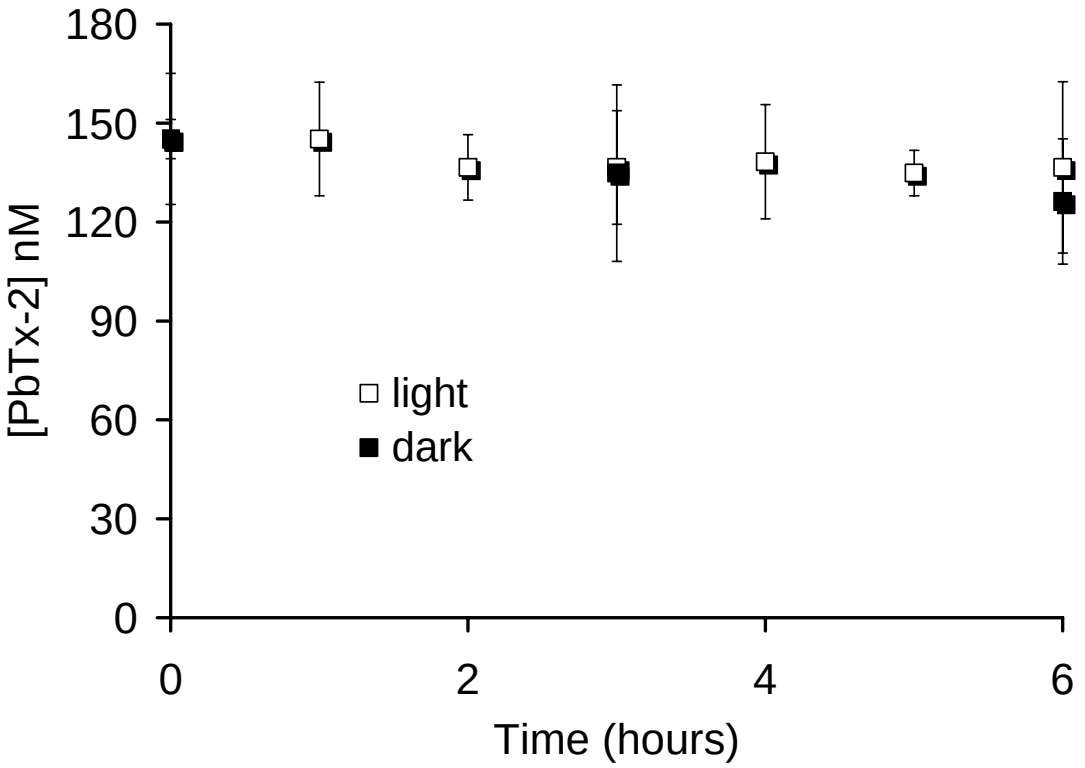

Figure 8: a) The concentration of light exposed and dark control samples of PbTx-2 in UV-oxidized, filtered, trace metal clean WBSW vs. time in a representative experiment. Error bars represent one standard deviation of 3 injections of each sample. Salinity 34, pH 8.1, temperature 25 ºC.

Effect of Oxygen on Photodegradation of PbTx-2

A series of experiments was carried out to determine the effect of oxygen and reactive oxygen species on the photodegradation of PbTx-2. In all experiments PbTx-2 was degraded virtually completely after 1 h of exposure and remained at non-detectable to very low concentrations for the entirety of the 6 h exposure (Figure 8). Dark controls showed little to no degradation over the course of the experiment. The average rate of three photolysis runs at which PbTx-2 degrades over the first hour in deoxygenated WBSW was 0.1 μmo1 h^{-1}.

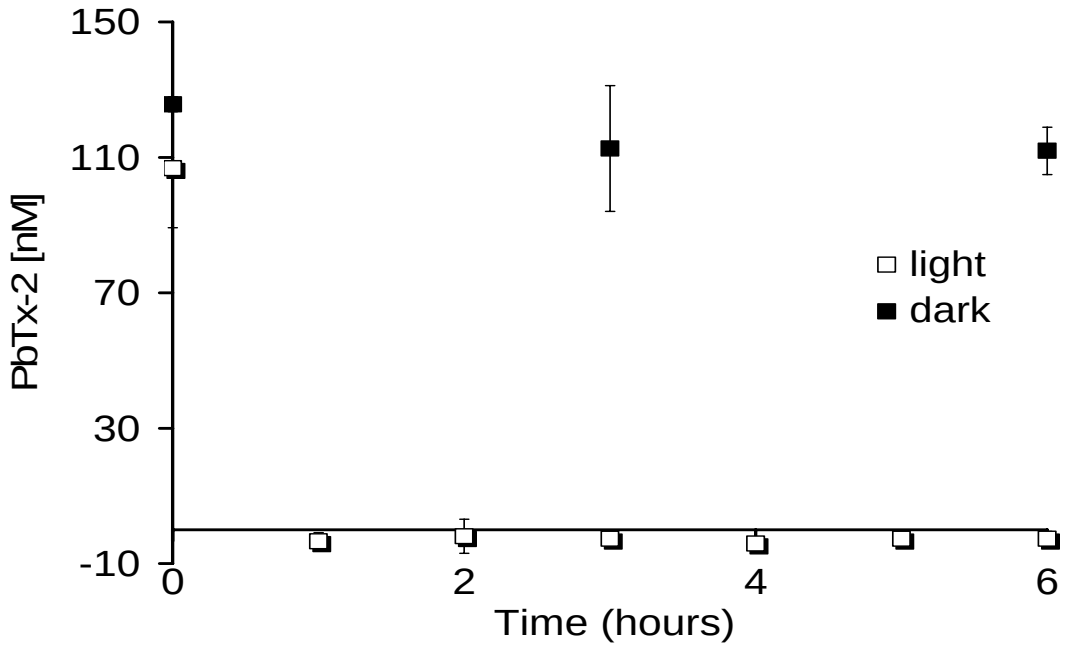

Figure 9: Concentration of light exposed and dark control samples of PbTx-2 in deoxygenated 0.2 μm-filtered Wrightsville Beach seawater as a function of irradiation time of one representative experiment. Error bars represent one standard deviation of 3 injections of each sample. 25 ºC; Salinity 34: pH 8.15.

An additional deoxygenated photolysis was carried out with a mixture of the most common brevetoxins found in natural bloom events. The following experiment was only conducted once with very few data points, therefore these results should only be regarded as preliminary. The brevetoxins used in this experiment were PbTx-1 (MW = 866), PbTx-2 (MW = 894), PbTx-3 (MW = 896), PbTx-6 (MW = 910), and PbTx-9 (MW = 898). In deoxygenated WBSW, all toxins degraded to very low concentrations within the first 3 h of exposure to simulated sunlight except PbTx-9. PbTx-9 degraded by approximately 80% after 6 h of exposure (Figure 9a). Dark controls showed little to no degradation. In oxygenated WBSW, PbTx-6 and PbTx-9 degraded twice as slowly compared to PbTx-1, 2, and 3 (Figure 9b). PbTx-1, 2, and 3 degraded at rates similar to prior experiments in untreated filtered WBSW (Table 5).

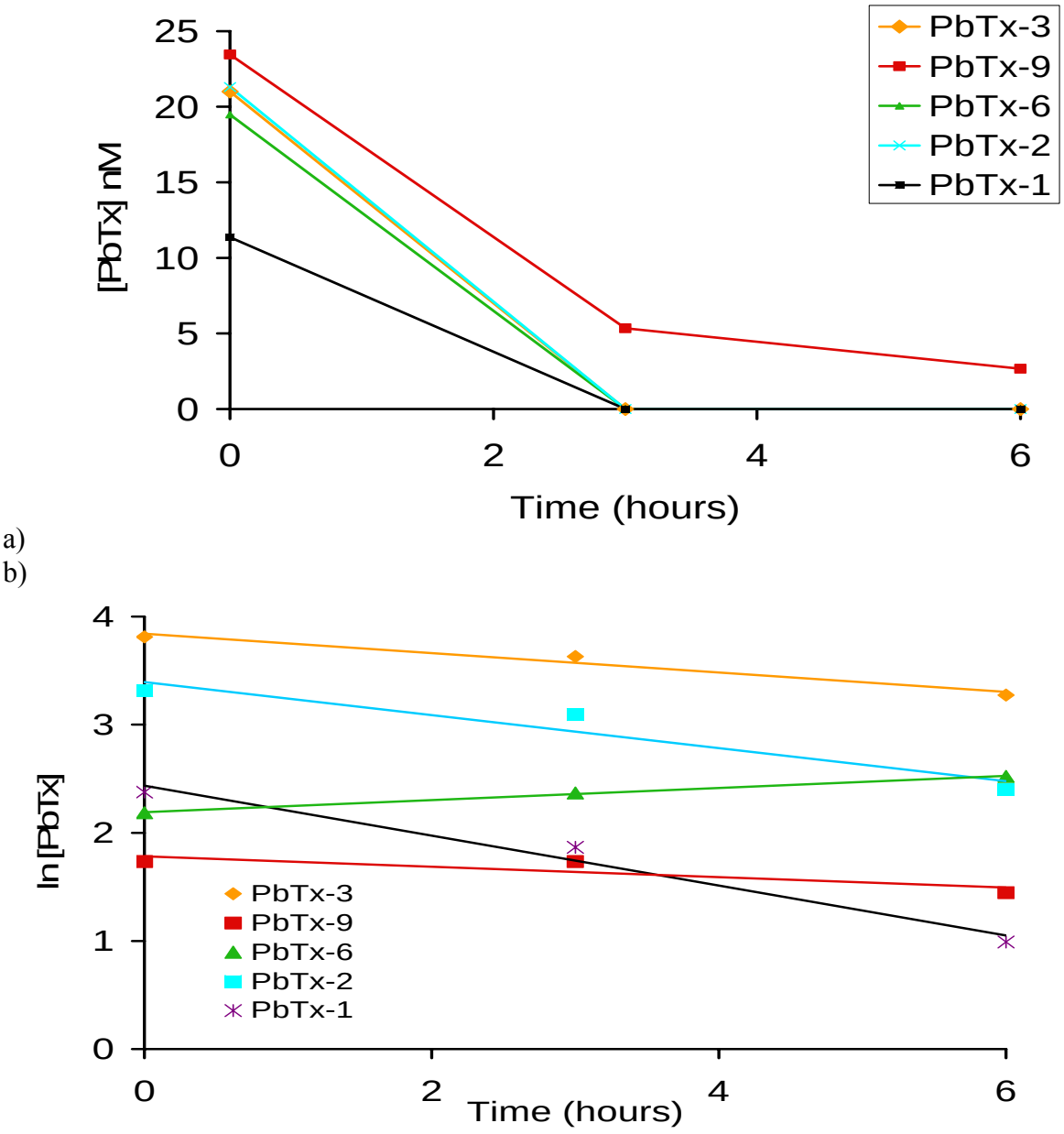

Figure 10: a) Concentration of light exposed samples in deoxygenated 0.2 µm-filtered Wrightsville Beach seawater as a function of irradiation time (hours) in one representative experiment. b) Natural logarithm of PbTx concentrations (PbTx-1, 2, 3, 6, 9) as a function of time in untreated filtered WBSW.

Table 5. Pseudo-first order rate constants of light exposed brevetoxins in untreated 0.2 μm-filtered WBSW. The goodness of fit (R^2) is also shown for each plot of natural logarithm as a function of irradiation time. All samples were irradiated for 6 hours under simulated sunlight at 25 ºC.

Toxin	**MW**	**Rate constant (h^{-1})**	**R^2**
PbTx-1	867	0.18	0.99
PbTx-2	894	0.16	0.94
PbTx-3	896	0.13	0.96
PbTx-6	910	0.02	0.97
PbTx-9	898	0.04	0.99

Rate of PbTx-2 adsorption onto particles

In order to determine the rate of adsorption of PbTx-2 onto particles, PbTx-2 was spiked into a sample of filtered and unfiltered WBSW and placed in the dark. The average loss of PbTx-2 onto particles in unfiltered WBSW of three experiments was 0.02 ± 0.002 whereas there was no loss of PbTx-2 in filtered WBSW (Figure 10). Although there was loss of PbTx-2 onto particles, the rate constant of particle adsorption is an order of magnitude less than loss due to photodegradation.

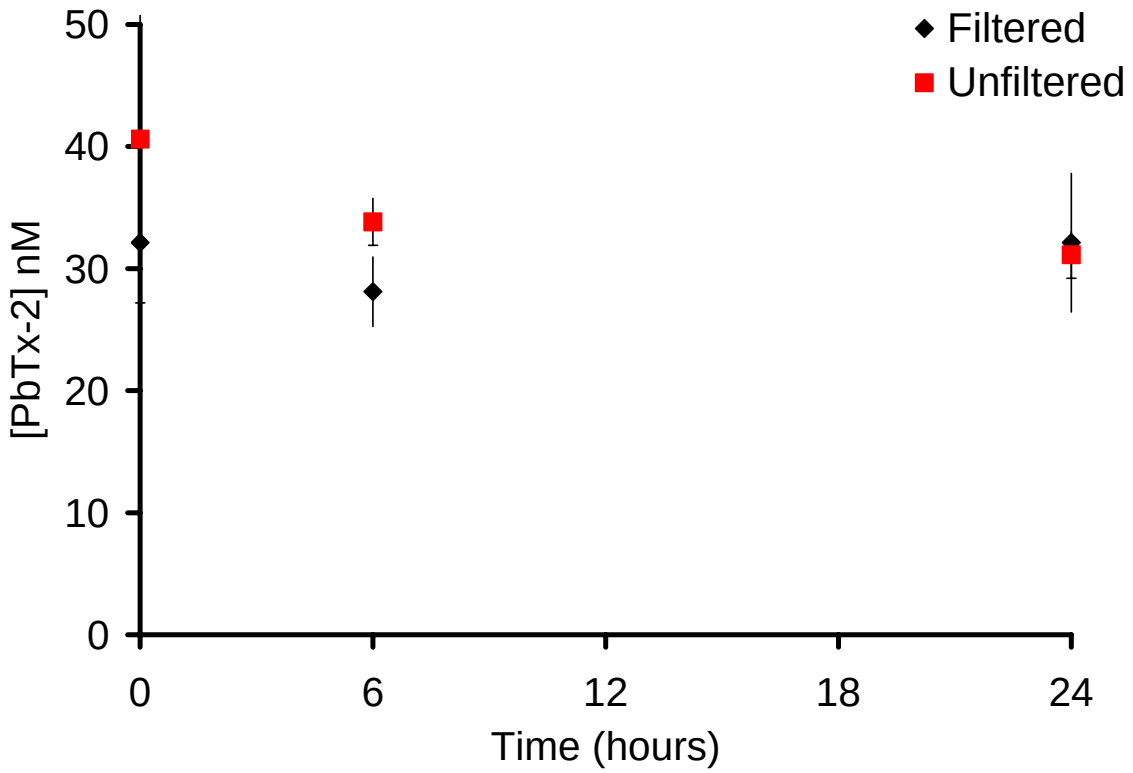

Figure 11. The loss of PbTx-2 onto particles in the dark as a function of time in unfiltered and filtered WBSW. The loss of PbTx-2 to particles in unfiltered water is $k_{unf} = 0.02 \pm 0.002\ h^{-1}$.

DISCUSSION

The average rate constant of PbTx-2 photodegradation was $0.2 \pm 0.05\ h^{-1}$ in filtered untreated WBSW exposed to simulated sunlight. A series of experiments were conducted following this to assess which environmental factors affected the rate of degradation. The first assessment was to observe the effect of the removal of chromophoric dissolved organic matter (CDOM) by UV oxidation. Irradiated CDOM leads to photoexcitation of molecules through energy transfer that are then available to react with other compounds. These photosensitized reactions can rapidly increase light-induced transformation of compounds that are otherwise stable in sunlight (Zepp et al. 1985). Photosensitizers are short-lived (10 ns or less) in singlet excited states; however, these molecules undergo intersystem crossing to excited triplet states. Triplet states of photosensitizers are relatively longer lived and thereby may transfer energy to ground state, to dioxygen, or another reaction which quenches this energy. Zepp et al. (1985) discussed the latter energy transfer to dienes such as polycyclic aromatic hydrocarbons which resemble brevetoxins. The energy required to excite dioxygen to its singlet state (94 kJ/mol) is well below triplet state energies of dienes (250 kJ/mol), therefore this energy is readily available to triplet state acceptors (Zepp et al. 1985).

The rate constant of PbTx-2 in UV-oxidized, filtered WBSW slowed significantly when CDOM was removed from the sample matrix. Furthermore, the removal of trace metals and CDOM led to no degradation of PbTx-2. These results suggest that both CDOM and trace metals are involved in the photochemical degradation of PbTx-2. It is well known that redox-active trace metals such as Cu^{2+} and Fe^{3+} can form complexes with humic acids and CDOM which subsequently take part in photochemical reactions (Zafiriou et al. 1984). It is suggested that the excitation of a metal chelated chromophoric dissolved organic matter complex (CDOM-m)*, where (CDOM-m) represents CDOM complexed by a metal in an excited state (denoted by

an asterisk), present in natural seawater photosensitizes PbTx-2 and initiates its photodegradation.

Hardman (2003) suggested that one of the possible mechanisms by which brevetoxin degrades is through photochemical intermediates such as oxygen radicals. Upon the absorption of UV radiation by DOM in natural waters, oxygen converts to several reactive oxygen species including singlet oxygen ($^1O_2$), superoxide and hydroperoxide (O^-_2 and HO_2), hydroxyl (OH^-) and peroxide (H_2O_2) (Zepp et al. 1985; Kieber et al. 2003; Cooper et al. 2007). In the series of photolyses in which filtered WBSW was deoxygenated, it was found that O_2 radicals and its intermediates were not responsible for degrading PbTx-2. As seen in Figure 8, PbTx-2 degraded almost immediately upon exposure to simulated sunlight to non-detectable or very low concentrations. Meanwhile, dark controls prepared in deoxygenated WBSW showed no degradation. Molecular oxygen quenches sensitizers, in this case (CDOM-m),* by energy transfer from triplet-state oxygen to singlet-state oxygen (Turro 1978).

$$(\text{CDOM-m})^* + {}^3O_2 \rightarrow \text{CDOM-m} + {}^1O_2$$

Oxygen was removed causing PbTx-2 to degrade more rapidly, thereby suggesting that O_2 species quenched energy transferred from (CDOM-m)* in the presence of sunlight. It is hypothesized that in the presence of oxygenated seawater, (CDOM-m)* photosensitizes both PbTx-2 and oxygen. In the absence of oxygen, (CDOM-m)* only reacts with PbTx-2 thereby rapidly increasing its photodegradation. In the presence of oxygen, (CDOM-m)* rapidly reacts with photoproduced intermediates, leaving little energy to attack PbTx-2. The involvement of (CDOM-m)* and trace metals in the degradation mechanism suggests that PbTx-2 degrades by a secondary photochemical pathway. Based on the results of Figures 4 through 8, the following mechanism is proposed for the photodegradation of PbTx-2 in WBSW.

1) CDOM-m + hv → (CDOM-m)*
2) PbTx-2 + (CDOM-m)* → CDOM-m + PbTx-2

3) $(CDOM\text{-}m)^* + {}^3O_2 \rightarrow {}^1O_2 + CDOM\text{-}m$

It is proposed that Eq. 3 is in direct competition with Eq. 2 to react with PbTx-2. The removal of oxygen (Eq. 3) from this system allows (CDOM-m)* to become more available to react with PbTx-2 thereby rapidly increasing the photodegradation of PbTx-2 by a secondary photochemical pathway.

Implications

The relevance of this study can be best understood if applied to a model in coastal seawater. To apply the information found here to an *in situ* bloom event, a model is proposed based on the determined rate constant of PbTx-2 in untreated filtered WBSW. A typical bloom can span an area of 400 square miles in the Gulf of Mexico with a concentration range of 10-100 $\mu g\ L^{-1}$ (Pierce et al. 2007). Applying the half life ($t_{1/2}$=3.2 hours) of PbTx-2 determined in this study to natural waters, PbTx-2 could potentially degrade by 75% within 6 h of exposure in the photic zone. The research here suggests that the photosensitized degradation of PbTx-2 is an important pathway that strongly affects the residence time of these toxins in natural bloom events. This is a preliminary estimate because it does not take into account factors such as attenuation of light within the water column, effects of particles, and other photolysis reactions.

In future studies, other factors to consider in assessing the role of photodegradation as a fate of brevetoxins in bloom events are adsorption to particles, sedimentation, and the ratio of intracellular to extracellular toxins. Due to the lipophilicity of these toxins, loss to particles of extra-cellular toxins is considered one of the primary fates in the water column (Pierce et al. 2001). The research here agrees with prior studies, but shows that photochemistry may be an even more important fate of brevetoxins in the water column and should be further studied as an influential factor in bloom dynamics. Recent research has shown that the most abundant intracellular toxin in bloom situation is PbTx-2, whereas the most abundant extra-cellular toxin is

PbTx-3 (Pierce et al. 2007). Pierce et al. (2007) found that as blooms progressed, the ratio of PbTx-3 to PbTx-2 increased, thereby indicating the conversion of PbTx-2 to PbTx-3 as cells die and lyse. In previous studies, the reduction of the PbTx-2 aldehyde to the PbTx-3 alcohol was attributed to enzymatic activity (Poli et al. 2000). It is important to further investigate trends in concentration and composition of the various toxins during bloom progressions in order to better understand composition, toxicity, and residence time of brevetoxins in the water column, benthic environment, and aerosols. A more comprehensive knowledge of these factors will allow for more precise prediction, monitoring, and awareness to help protect marine life, as well as human health in future red tide events.

LITERATURE CITED

Backer, L., B. Kirkpatrick, L. Fleming, Y. Cheng, R. Pierce, J. Bean, R. Clark, D. Johnson, A. Wanner, R. Tamer, Y. Zhou and D. Baden. (2005). "Occupational Exposure to Aerosolized Brevetoxins during Florida Red Tide Events on a Healthy Worker Population." Environmental Health Perspectives **113**: 644-9.

Backer, L. C., L. E. Fleming, A. Rowan, Y.-S. Cheng, J. Benson, R. H. Pierce, J. Zaias, J. Bean, G. D. Bossart, D. Johnson, R. Quimbo and D. G. Baden (2003). "Recreation exposure to aerosolized brevetoxins during Florida red tide events." Harmful Algae **2**: 19-28.

Baden, D. G., A. J. Bourdelais, H. Jacocks, S. Michelliza and J. Naar (2005). "Natural and Derivative Brevetoxins: Historical Background, Multiplicity and Effects." Environmental Health Perspectives **113**: 621-625.

Baden, D. G., L. E. Fleming and J. A. Bean (1995). "Marine Toxins." Handbook of Clinical Neurology **21**: 1-34.

Baden, D. G., T. J. Mende, G. Bikhazi and I. Leung (1982). "Toxicity of two toxins from the Florida red tide marine dinoflagellate, *Ptychodiscus brevis*." Toxicon **20**: 929-932.

Baden, D. G. and Tomas, C.R. (1989). "Variations in major toxins composition for six close of *Ptychodiscus brevis*." Environmental Science and Toxicology: 415-418.

Bossart, G. D., Baden, D.G., Ewing, R., Roberts, B., and Wright, S. (1998). "Brevetoxicosis in manatees (*Trichechus manatus latirostris*) from the 1996 epizootic; gross, histopathologic and immunocytochemical features. ." Toxins Pathology **26**: 276-282.

Bouillon, R. C., T. Knierim, R. Kieber, S. Skrabal and J. Wright (2006). "Photodegradation of the algal toxin domoic acid in natural water matrices." Limnol. Oceanogr. **51**: 321-330.

Bourdelais, A., H. Jacocks, J. Wright, P. Bigwarfe and D. G. Baden (2005). "A New Polyether Ladder Compound Produced by the Dinoflagellate *Karenia brevis*." Journal of Natural Products. **68**: 2-6.

Cheng, Y., Y. Zhou, M. I. Clinton, R. Pierce, J. Naar, L. Backer, L. Fleming, B. Kirkpatrick and D. G. Baden (2005). "Characterization of Marine Aerosol for Assessment of Human Exposure to Brevetoxins." Environmental Health Perspectives **113**: 638-643.

Cooper, W., A. Jones, R. F. Whitehead and R. Zika (2007). "Sunlight-Induced Photochemical Decay of Oxidants in Natural Waters: Implications in Ballast Water Treatment." Environmental Science Technology **41**: 3728-3733.

de Mora, S. d., S. Demers and M. Vernet (2000). The effects of UV radiation in the marine environment, Cambridge University Press: 318.

Forrester, D. J., J. M. Gaskin, F. H. White, N. O. Thompson, J. A. Quick, G. E. Henderson, J. C. Woodard and W. D. Robertson (1977). "An epizootic of waterfowl associated with a red tide episode in Florida." Journal of Wildlife DIstribution **13**.

Gawley, R. E., K. S. Rein, G. Jeglitsch, D. J. Adams, E. A. Theodorakis, J. Tiebes, K. C. Nicolaou and D. G. Baden (1995). "The relationship of brevetoxins 'length' and A-ring functionality to binding and activity in neuronal sodium channels." Chemistry & Biology **2**: 533-541.

Hua, Y. and R. B. Cole (2000). "Electrospray Ionization Tandem Mass Spectrometry for Structural Elucidation of Protonated Brevetoxins in Red Tide Algae." Analytical Chemistry **72**: 376-383.

Jeglitsch, G., K. S. Rein, D. G. Baden and D. J. Adams (1998). "Brevetoxin-3 (PbTx-3) and its dervatives modulate single tetrodotoxin-sensitive sodium channels in Ra sensory neurons." Journal of Pharmacological Experimental Therapeutics. **284**: 516-525.

Kieber, D. J., B. M. Peake and N. M. Scully (2003). Reactive Oxygen Species in Aquatic Ecosystems. Comprehensive Series in Photochemistry & Photobiology. D. P. Hader and G. Jori. Cambridge, U.K., The Royal Society of Chemistry. **1:** 251-288.

Kirkpatrick, B., Lora E. Fleming and L. C. Backer (2004). "Literature review of Florida red tide: implications for human health effects." Harmful Algae **3**: 99-115.

Lin, Y. Y., M. Risk, S. M. Ray, D. Van Engen, J. Clardy and J. Golik (1981). "Isolation and structure of brevetoxin B from "red tide" dinoflagellate *Gymnodium breve (Ptychodiscus)*." Journal of American Chemical Society **103**: 6773-6776.

Mill, T. (1999). "Predicting Photoreaction Rates in Surface Waters." Chemosphere **38**: 1379-1390.

Pierce, R. H., M. Henry and P. Blum (2007). "Brevetoxin abundance and composition during ECOHAB-Florida field monitoring cruises in the Gulf of Mexico." Continental Shelf Research.

Pierce, R. H. and G. J. Kirkpatrick (2001). "Innovative techniques for harmful algal toxin analysis." Environmental Toxicology and Chemistry **20**: 107-114.

Pierce, R. H. and G. J. Kirpatrick (1986). "Red Tide (*Ptychodiscus brevis)* toxin aerosols: a review." Toxicon **24**: 955-965.

Pierce, R. H. H., M.S., Blum, P.C., Lyons, J., Cheng, Y.S., Yazzie, D., and Zhour, Y. (2003). "Brevetoxin concentrations in marine aerosol: human exposure levels during a *Karenia brevis* harmful algal bloom." Bulletin of Environmental Contamination & Toxicology **70**: 161-165.

Plakas, S., Z. Wang, K. El Said, E. Jester, H. Granade, L. Flewelling, P. Scott and R. Dickney (2004). "Brevetoxin Metabolism and Elimination in the Eastern Oyster (Crassostrea virginica) after controlled exposures to Karenia brevis." Toxicon **44**: 678-85.

Poli, M. A., T. J. Mende and D. G. Baden (1986). "Brevetoxins, unique activators of voltage sensitive sodium channels, bind to specific sites in rat brain synaptosomes." Molecular Pharmocology **30**: 129-135.

Poli, M. A., S. M. Musser, R. W. Dickey, P. P. Eilers and S. Hall (2000). "Neurotoxic shellfish poisoning and brevetoxin metabolites: a case study from Florida." Toxicon **38**: 981-993.

Purkerson-Parker, S. L., L. Fieber, K. S. Rein, T. Podana and D. G. Baden (2000). "Brevetoxin derivatives that inhibit toxin activity." Chemical Biology **7**: 385-393.

Rein, K. S., D. G. Baden and R. E. Gawley (1994). "Conformational analysis of the sodium channel modulator brevetoxin a, comparison with brevetoxin b conformations, and an hypothesis about the common pharmacophore of the "site 5" toxins." Journal of Organic Chemistry **59**.

Rein, K. S. and J. Borrone (1999). "Polyketides from dinoflagellates: origins, pharmacology and biosynthesis." Comparative Biochemistry and Physiology Part B: Biochemistry and Molecular Biology **124**: 117-131.

Shimizu, Y., S. Gupta and A. V. K. Prasad (1990). Biosynthesis of dinoflagellate toxins. Toxic Marine Phytoplankton. E. Graneli, B. Sundstrom, L. Edler and D. M. Anderson. New York, Elsevier**:** 62-76.

Trainer, V. L., D. G. Baden and W. A. Catterall (1994). "Identification of the peptide components of the brevetoxin receptor site of rat brain sodium channels." Journal of Biological Chemistry **269**: 19904-19909.

Turro, N. J. (1978). Modern Molecular Photochemistry. Reading, The Benjamin/Cummings Publishing Co., Inc.

Welker, M. and C. Steinberg (2000). "Rates of Humic Substance Photosensitized Degradation of Microcystin-LR in Natural Waters " Environmental Science and Technology **34**: 3415-3419.

Zafiriou, O., J. Joussot-Dubien, R. Zepp and R. Zika (1984). "Photochemistry of natural waters." Environmental Science and Technology **18**: 358A-371A.

Zepp, R., P. Schlotzhauer and R. Sink (1985). "Photosensitized transformations involving electronic energy transfer in natural waters: Role of humic substances." Environmental Science and Technology **19**: 74-81.

APPENDIX

Sample Extraction

The purpose of extraction for this study was to preconcentrate the photolyzed sample to approximately 100 µL for injection on HPLC or LCMS. The most efficient method of extraction was expected to be solid phase extraction (SPE). Liquid-liquid extraction was considered but sample volume lead us to assume SPE would be more practical. Three different eluents were tested: methanol, acetonitrile, and acetone. After washing the column with HPLC grade water, the sample was eluted with methanol or acetonitrile followed by acetone. For both primary eluents, sample remained in the secondary eluent, acetone. The volume that was necessary to recover most sample was simply too high. It was assumed that acetone was truly stripping the most sample from the cartridge therefore we eliminated the primary eluent and used acetone as the sole eluent. I found that the brevetoxin was removed from the cartridge more efficiently with a lower volume acetone than the original procedure. Another consideration was the type of cartridge was used. Three different types of cartridges were tested for best sample recovery including C8, C4, and C18. Although having only slightly better recovery, C18 cartridges collected a higher percentage of the original spiked concentration. One problem when it came to solid phase extraction was minimizing the amount of transfer vials. A beaker with 30 mL of medium grade seawater (collected from filtered ICW at CMS) was spiked with a known concentration of brevetoxin (approximately 2-4 µg). The sample was originally transferred from the beaker with a pipet to the cartridge. In order to minimize the surface area to which the brevetoxin may adhere. I decided to pour the spiked sample from the beaker directly into the SPE tube. Also, to ensure brevetoxin did not adhere to the beaker, I rinsed the original beaker with approximately 2 mL of acetone that was passed through the cartridge and collected in the final extracted vial.

During method development, several types of cartridges were used to determine optimal recovery. To evaluate each cartridge, a sample of 30 mL 0.2 μM filtered seawater was spiked with 1-5 μg PbTx-2. Each cartridge was first washed with 6 mL acetone to remove any impurities followed by 10 mL Milli-Q water to repolarize the cartridge. Samples were then passed through dropwise at approximately 1 mL min^{-1}, followed by 10 mL Milli-Q to remove salts. Various eluents were tested such as methanol, acetone, and acetonitrile. Each trial was analyzed on HPLC along with a standard serial dilution without breaking chromatography. Peak height and peak area were plotted against the standard curve. Percent recovery was calculated by dividing the extracted concentration by the actual concentration of the original solution. Ultimately, using 100% acetone as the sole eluent recovered the highest percentage toxin with minimum volume. Samples were collected in 10 mL glass vials until further analysis.

HPLC method

For HPLC analysis, an Agilent 1100 instrument with diode array detector was used for preliminary analysis. The optimal mobile phase that would be used for both HPLC and LCMS was determined by comparing resolution using mobile phase with and without modifiers. In past studies, Hardman (2003) used either 85:15 methanol:water or 70:30 acetonitrile:water. Both of these mixtures were tested on an Agilent 1100 HPLC. Unmodified acetonotrile:water was better than methanol:water with respect to peak signal. Increasing the percent organic solvent showed even better signal. The next step was to compare mobile phases with and without modifiers. A "naked" run of 98: 2 Acetonitrile: water was compared with 98:2 acetonitrile:water, 0.1% formic acid, 0.01% trifluoracetic acid. Mobile phase with modifiers yielded a peak with less fronting and tailing than the unmodified mobile phase. Peaks were analyzed by calculating half height, tailing, fronting, and symmetry. Two methods were verified both using the sample mobile phase: mobile phase A consisted of 98% HPLC grade water, 2% filtered acetonitrile (CAN), 0.1% formic acid, 0.01% trifluoracetic acid (TFA), and mobile phase

B consisted of 98% filtered ACN, 0.1% formic acid, 0.01% TFA. For Method 1, an isocratic gradient of 85%B, 15%A at 1 mL min^{-1} was passed through a reverse phase 2.0 x 150mm Phenomenex C18 column packed with 5 µm particles. For Method 2, a gradient (T=0 min, 60%A, T=8 min, 85% B for 15 min allowing 7 minutes for column equilibration) at 1 mL min^{-1} was used on a 2.0 x 50 mm phenyl-hexyl column. Injection volume for both methods was 5 µL. The Agilent 1100 was equipped with well-plate temperature control which was maintained at 4 ºC to prevent evaporation of solvent. PbTx-2 calibration solutions were prepared from the aforementioned stock solution to final concentrations of 1, 2.5, 5, and 10 ug mL^{-1}. Calibration standards were prepared fresh for each individual experimental run. A new calibration curve was created for each sample run and injected periodically throughout the run. Samples were then normalized to their respective standard curve injection to account for instrument drift. The level of quantitation was 1ug/mL on the Agilent 1100. Five blank samples were injected at the start of each run to allow for equilibration and system suitability. One blank was injected between each sample to avoid sample carryover.

The two methods mentioned previously for HPLC were transferred to a quadrapole QTrap LCMS. The two original methods were developed on an Agilent 1100 HPLC therefore needed to be scaled down.. For method 1, in which a 150 x 2.0 mm column was used, flow rate was decreased from 1.0 mL min^{-1} to 0.2 mL min^{-1} for injection onto the mass spectrometer. Flow rate was decreased from 1.0 mL min^{-1} to 0.2 mL min^{-1} for method 2 as well. The limit of quantitation was 0.1 ug mL^{-1} on the LCMS QTOF. The following MS settings were varied while injecting identical concentrations to elicit the lowest LOD and LOQ. These settings were found to work best with the LC method mentioned previously as well as the sample matrix.